Adaptive self-organization of Bali's ancient rice terraces

J. Stephen Lansing[a,b,c,e,1], Stefan Thurner[a,b,d,e,f], Ning Ning Chung[b,g], Aurélie Coudurier-Curveur[h], Çağil Karakaş[h], Kurt A. Fesenmyer[i], and Lock Yue Chew[b,g]

[a]Santa Fe Institute, Santa Fe, NM 87501; [b]Complexity Institute, Nanyang Technological University, Singapore 637723; [c]Stockholm Resilience Center, 104 05 Stockholm, Sweden; [d]Section for Science of Complex Systems, Medical University of Vienna, A-1090 Vienna, Austria; [e]Complexity Science Hub Vienna, A-1080 Vienna, Austria; [f]International Institute for Applied Systems Analysis, A-2361 Laxenburg, Austria; [g]School of Physical & Mathematical Sciences, Nanyang Technological University, Singapore 637371; [h]Earth Observatory of Singapore, Nanyang Technological University, Singapore 639798; and [i]Trout Unlimited, Boise, ID 83702

Spatial patterning often occurs in ecosystems as a result of a self-organizing process caused by feedback between organisms and the physical environment. Here, we show that the spatial patterns observable in centuries-old Balinese rice terraces are also created by feedback between farmers' decisions and the ecology of the paddies, which triggers a transition from local to global-scale control of water shortages and rice pests. We propose an evolutionary game, based on local farmers' decisions that predicts specific power laws in spatial patterning that are also seen in a multispectral image analysis of Balinese rice terraces. The model shows how feedbacks between human decisions and ecosystem processes can evolve toward an optimal state in which total harvests are maximized and the system approaches Pareto optimality. It helps explain how multiscale cooperation from the community to the watershed scale could persist for centuries, and why the disruption of this self-organizing system by the Green Revolution caused chaos in irrigation and devastating losses from pests. The model shows that adaptation in a coupled human–natural system can trigger self-organized criticality (SOC). In previous exogenously driven SOC models, adaptation plays no role, and no optimization occurs. In contrast, adaptive SOC is a self-organizing process where local adaptations drive the system toward local and global optima.

self-organization | criticality | irrigation | evolutionary games | Pareto optimality

The geometric precision of Balinese rice terraces has inspired generations of postcard photographers. Viewed from above, a changing mosaic of colors appears: green when the rice is young, yellow as it nears harvest, silver when the paddies are flooded, and brown when they are drained. These colors are not uniform across the island, because Bali is an equatorial island with only two seasons, wet and dry. Consequently, farmers can plant their crops at any time, although they avoid harvesting in the rainy season. The colored patches that make up the mosaics are visible in Google Earth. Like many natural phenomena, patches show a characteristic power-law distribution of sizes. However, in this case, the patches are created by the farmer's decisions about when to synchronize irrigation schedules with their neighbors: Each patch displays the outcome of these choices. Adjacent patches tend to be correlated. This correlation weakens with distance, a relationship that also follows a specific power law (Fig. 1). To discover why harvests approach a maximum when both the size distribution of patches and the corresponding correlation functions fit power-law distributions, we need a model that relates the decisions of the farmers to the consequences for irrigation flows and rice growth.

In Bali, water is regarded as a public good, the gift of the Goddess of the Lakes. Rice is grown in paddy fields fed by irrigation systems dependent on rainfall. Rainfall varies by season and, in combination with groundwater inflow, determines river flow. By virtue of their location, upstream farmers can influence

how much water reaches their downstream neighbors. Across the island, farmers recognize two management systems. In tulak sumur ("reject the wellspring"), everyone is free to plant whenever they like, which gives upstream farmers an advantage over their downstream neighbors. Alternatively, in kerta masa ("lawful/good timing"), farmers agree to adopt synchronized irrigation schedules.

Kerta masa is sustained by local water-user groups called subak, which have existed since the 11th century (1). Irrigation schedules are chosen by consensus in subak meetings. In prior research on a group of 10 subaks practicing kerta masa, we measured irrigation flows and found that they correlated perfectly with the agreed-upon irrigation schedules (*SI Appendix*, Fig. S3). Kerta masa tends to equalize rice harvests, and, in a typical survey, 39 of 40 farmers agreed that their harvests are about the same as those of their neighbors (*SI Appendix*, Table S1) (2). However, to sustain kerta masa, upstream farmers must give up their advantage in irrigation control. How, then, did it become the norm in Bali, whereas tulak sumur is regarded as a rare and problematic condition?

To find out, in prior research, we modeled the emergence of cooperation in a simple game involving only two rice farmers, one upstream from the other (2). We allow the upstream farmer to have first claim on any water in the system. To simplify

Significance

In Bali, the cooperative management of rice terraces extends beyond villages to whole watersheds. To understand why, we created a model that explores how cooperation can propagate from pairs of individuals to extended groups, creating a resilient system of bottom-up management that both increases and equalizes harvests. Spatial patterns of collective crop management—observable in Google Earth—closely match the predictions of the model. The spatial patterning that emerges is nonuniform and scale-free. Although the model parameters here are tuned to Bali, similar mechanisms of emergent global control should be detectible in other anthropogenic landscapes using multispectral imagery. Recognizing this signature of emergent system-wide cooperation may help planners to avoid unproductive changes to successful bottom-up systems of environmental management.
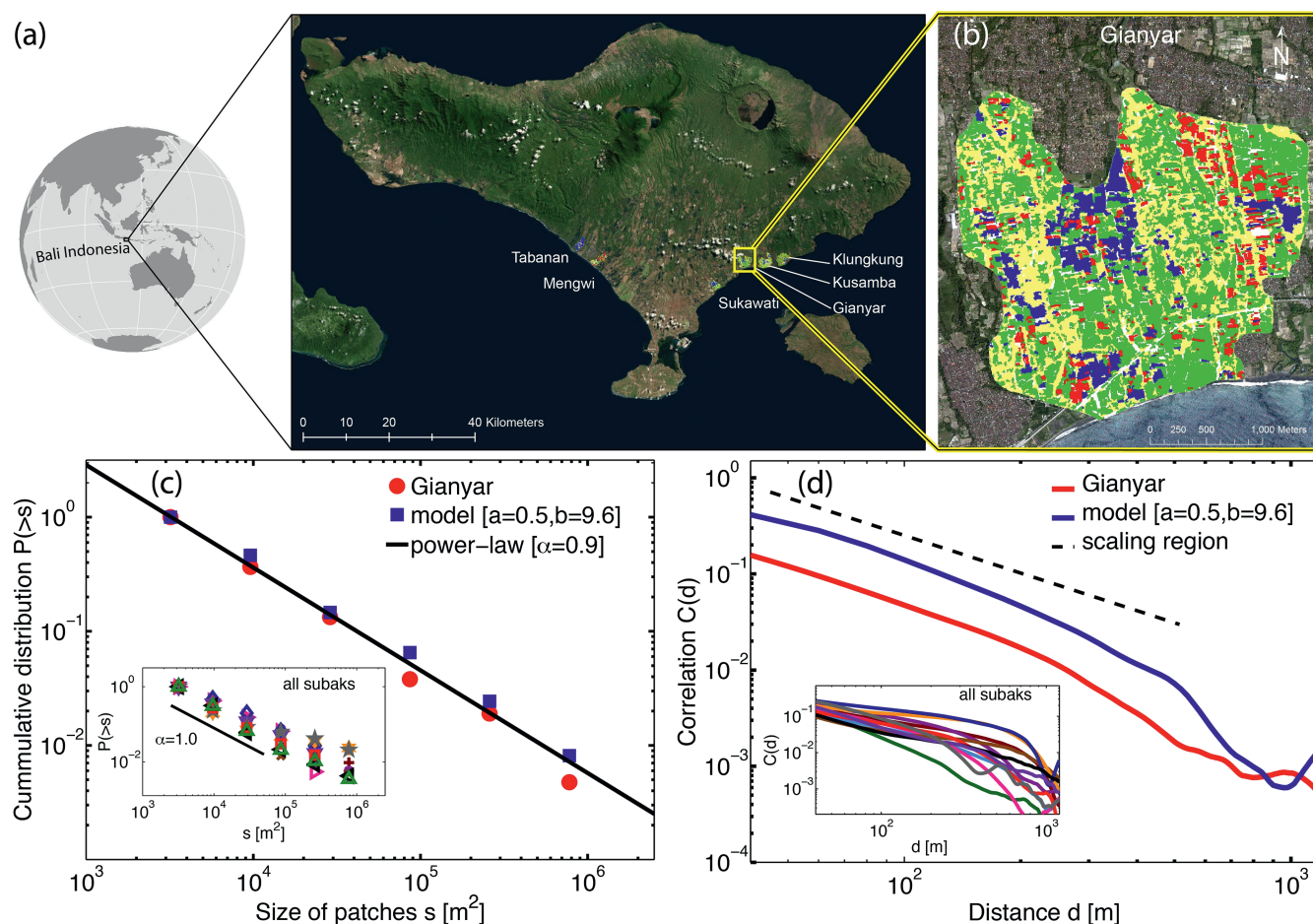
Fig. 1. (A) Location of study sites: six randomly selected rice-growing regions of Bali. Photosynthetic activity was analyzed using multispectral and panchromatic satellite images to classify four stages of rice growth in the terraces, which appear as differently colored patches. (B) Image analysis of rice growth (indicating synchronized irrigation schedules in the region of Gianyar). The four colors of the patches indicate the four stages: growing rice (yellow), harvest (green), flooded (red), drained (blue). (C) Cumulative distribution of the patch sizes $P(>s)$ for Gianyar (red circles) and for our model results (blue squares). (*Inset*) All 13 observations at the six regions, indicating power-law behavior, with an exponent around $\alpha \approx 1$. (D) Correlation functions $C(d)$ of the image (planting regions only) as a function of distance for Gianyar (red) and the model (blue). The slow decay (power law) indicates long-range correlations, or "system-wide connectivity" of patches. (*Inset*) All 13 observations. See *SI Appendix* for details.

matters, suppose that the farmers must choose one of two possible dates, A or B, on which to plant their crops. We assume that the water supply is adequate to accommodate the needs of one farmer during any given period but is insufficient if both decide to plant simultaneously. The maximum harvest is 1. Let δ $(0 < \delta < 1)$ give the crop loss due to reduced water inputs experienced by the downstream farmer if he plants at the same time as the upstream farmer. However, harvests are also affected by rice pests (3). If the farmers plant at different times, they will harvest at different times. This schedule provides an opportunity for rice pests to migrate between the fields. Let ρ $(0 < \rho < 1)$ give the crop loss due to pest migration between the fields under these conditions (for simplicity, we assume that there is no pest damage if the crops are planted simultaneously).

If the upstream farmer is not very worried about damage from pests, he will have little incentive to synchronize his irrigation schedule with the downstream farmer. This situation results in a mixed strategy (one player chooses A and the other chooses B), corresponding to tulak sumur. The expected aggregate crop yield for both farmers from the mixed strategy is $2 - \delta/2 - \rho$. When $\rho > \delta/2$, both farmers will obtain better harvests by cooperating in a single irrigation strategy (either A or B). This agreement holds because pest damage is borne by both farmers whereas water damage impacts only the downstream farmer; thus aggre-

gate yields increase by coordinating when pest damage is at least half as bad as water damage. In this case, corresponding to kerta masa, it is in the individual interest of both farmers to cooperate (formally, this is known as a coordinated equilibrium).

Thus, the threat of increased pest damage from downstream neighbors provides an incentive for upstream farmers to synchronize their irrigation schedules. We tested the salience of this incentive in a survey of 150 farmers in 10 subaks, to whom we posed the question, "Which is worse, pest damage or irrigation water shortages?" In each subak, five farmers were selected whose fields are located in the upstream part of their subak, five more from the middle of the subak, and the last five from the downstream area of the subak. The results showed that upstream farmers worry more about pests, whereas downstream and middle farmers are more concerned with water shortages (Pearson χ^2 14.083, $P < 0.001$) (2).

Thus, in the two-player game, whether cooperation emerges depends on the trade-off between pest damage ρ and water shortages δ, both of which are fixed and known to the players in advance. In reality, for any farmer, ρ depends on both the intrinsic capacity of endemic pests to cause damage and whether neighboring farmers choose to control the pests by synchronizing irrigation. Similarly, δ depends on both the inflow of irrigation

water into the subak and the scale at which groups of farmers synchronize irrigation. Consequently, the pest–water trade-off for each farmer varies depending on where his farm is located and the outcome of the irrigation schedules chosen by his neighbors. Whether both farmers choose to cooperate (synchronize irrigation) depends on the magnitude of ρ and δ.

To explore how patterns of irrigation scheduling emerge from this mutual dependence, we created an adaptive version of the game in which farms are embedded on the sites of an $L \times L$ lattice, with dimension $L = 100$. Parameters a and b specify the relative weights of pest and water stress, respectively, for the entire lattice and are set in advance. The lattice represents a rice-growing region such as shown in Fig. 1B.

This model proceeds through a process of trial-and-error adaptation. Losses from water stress are calculated based on the distribution of irrigation schedules for the entire lattice: The fewer the farmers following a given schedule, the more water they have to share. However, this reward for asynchronous irrigation is balanced by the need to reduce losses from pests, which depends on the fraction of neighboring farmers (f_p) within a given radius (r) that synchronize their irrigation schedules. When pest damage is at least half as bad as water damage, does cooperation spread and do aggregate harvest yields increase?

The model is initialized with random irrigation patterns for all sites at $t = 0$, when every farmer i chooses one of four possible irrigation schedules C_i with probability $1/4$. At the end of a time step (representing one simulated irrigation cycle), each farmer compares his harvest with those of his closest neighbors, and uses this information to choose his irrigation schedule for the next cycle (Fig. 2). Because the farmers do not know ρ and δ in advance, they must guess. Anticipating future pest outbreaks or water shortages is challenging, and the actual decision-making process in subaks typically involves lengthy discussions (3, 4). Irrigation flows along the tiny canals that connect adjacent fields are also complex, involving bargains similar to the game described above. We do not attempt to replicate this level of complexity in the model. Instead, we implement very simple strategies to discover whether they are sufficient to enable successful adaptation (Fig. 2). Once the decision rule and the background pest and water levels are determined, the model proceeds in the following steps:

i) Assume we are at the beginning of time step $t + 1$. Calculate the rice harvest for each individual farmer i by debiting his losses from pest damage and water stress, according to $H^i(t+1) = H_0 - a/0.1 + f_p^i(t) - b f_w^i(t)$, where H_0 is a con-

stant representing the initial harvest before loss. Here $f_p^i(t)$ denotes the fraction of neighbors of farmer i within a radius r who share the same cropping pattern as i at the previous time step t, which reduces local pest damage, and $f_w^i(t)$ is the fraction of all lattice sites that have the same cropping pattern as i. The number 0.1 in the formula is to ensure that H_i is positive. The parameters a and b specify the relative weights of the pest loss and water stress, respectively. We set $H_0 = 5$ and $r = 2$ (lattice units) for all simulations. Details are provided in *SI Appendix*.

ii) Pick one specific farmer i randomly.

iii) Farmer i compares his harvest $H^i(t+1)$ with the harvests of his four nearest neighbors and copies the irrigation schedule of one or more neighbors according to the decision rule (Fig. 2). In the simplest case, it is the neighbor who had the best harvest in the previous irrigation cycle j: $C_i(t+1) = C_j(t)$ (Fig. 3). For an explanation of the reasons for the difference between these decision rules and the game, see *SI Appendix, Game and Lattice Models*.

iv) Pick next farmer until all are updated (synchronously).

v) For a small fraction of lattice sites, the irrigation schedules are randomly updated, to simulate empirically observed nonconformity (see *SI Appendix*).

vi) Perform the next time step.

vii) Repeat for more time steps until harvests converge to maximum.

Model Results

The model evolves through a process of trial-and-error adaptation by the farmers. At first, in the initial random state ($t = 0$), the correlation between farms is close to zero (Fig. 3A). What happens next depends on the ecological parameters pests (a) and water stress (b), and on the decision rule followed by the farmers. There are three trivial attractors ("phases") (*SI Appendix,* Fig. S4): (*i*) If water stress is negligible ($b \ll 1$) eventually all farms adopt the same irrigation schedule to control pests, resulting in a single uniform patch that spans the entire lattice. (*ii*) If $b > 20a$, water stress dominates, and many small patches appear; this increases the variance of irrigation schedules, reducing water stress, but allows pests to migrate between adjacent patches. (*iii*) For $b < 20a$, after a very long transient phase (thousands of cycles), a quadrant state is reached that separates the lattice into four quadrants with the same irrigation schedules.

The fourth attractor, which is nontrivial, emerges at the phase transition, exactly at the boundary where the water and pest stress phases equalize. Correlation lengths increase as the cycles of planting and harvest progress, and farms coalesce into small, irregularly sized patches with identical irrigation schedules. Patches form very quickly, as seen in Fig. 3A, and soon become large enough to dramatically reduce pest damage. Uniformly short correlation distances indicate that the patches are functionally independent: Each patch discovers its own solution to the pest–water trade-off. Rice harvests improve rapidly within the first time steps, and correlations between farms increase. However, there is still some variation in harvests, so farms on the borders of the patches continue to experiment with different irrigation schedules. Adaptation ceases when no farm can improve its harvest by changing its irrigation schedule. The geographic scale at which the pest–water trade-off is solved shifts from many small independent patches (small correlation length) to the entire lattice by ($t = 10$), equivalent to 5 y of double cropping. Subsequently there is little change: At $t = 400$, the situation is very similar to $t = 10$. In Fig. 3B, we study the average harvest $H = 1/L^2 \sum_{i=1}^{L^2} H^i$ as a function of simulation time steps (blue line, maximum strategy). We see that the maximum of H is reached very soon.
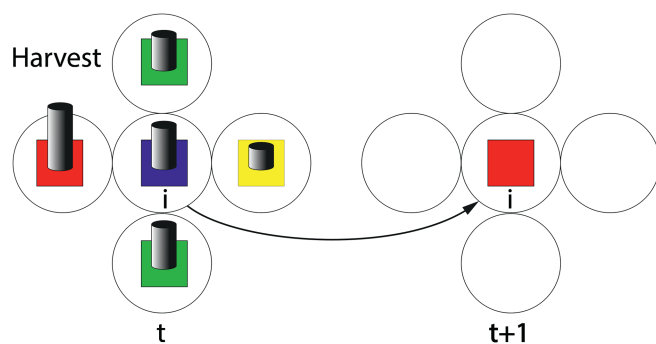

Fig. 2. Update rule for farmer *i*. Colors denote irrigation schedules. For example, green might signify planting in January, and blue might signify planting in March. At time $t + 1$, farmer i compares his harvest with those of his four closest neighbors at time t. Because the red schedule produced the best harvests, he adopts it for the next cycle. This update corresponds to step iii in the model.
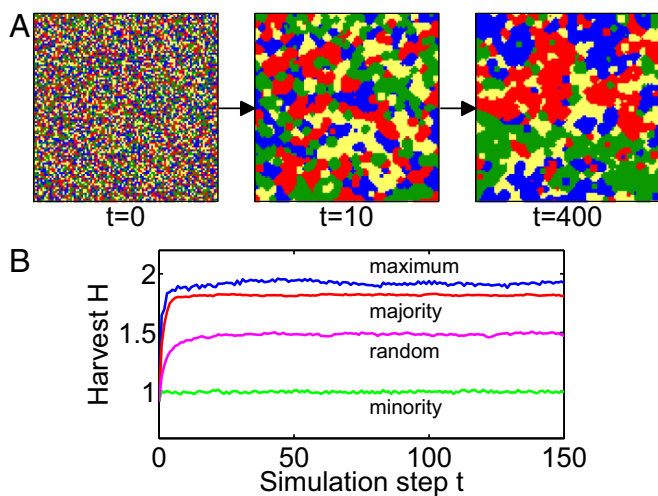
Fig. 3. (*A*) Evolution of the irrigation schedules from an initial random configuration at $t = 0$ to $t = 10$, whereupon patch sizes become power-law distributed. At $t = 400$, the irrigation patterns have changed very little and approach a long-lived steady state distribution (see *SI Appendix*). (*B*) Effect of decision rules on harvests. For the "maximum" rule (step *iii*, where farmers choose the best harvest in their neighborhood), average harvests rapidly increase as patch distributions shift to the power-law distribution (blue line). A similar rapid increase occurs for the "majority" update strategy, where farmers copy the schedule of the majority (red). To copy a random neighbor's irrigation schedule is the "random" strategy (pink) that leads to inferior harvests. Extending this logic, when farmers update according to the minority of their neighbors, harvests do not improve. The maximum possible harvest is $H = H_0 = 5$ in the absence of pest or water stress. In the simulation shown, both pest and water stress are strongly present, $a = 0.5$ and $b = 9.6$.

In summary, cooperation quickly spans the entire lattice. Harvests tend to increase and equalize, approaching Pareto optimality at the phase transition where both the frequency distribution of synchronized irrigation patches and the correlations between them become power laws. (Pareto optimality is a state of resource allocation from which it is impossible to reallocate so as to make any individual better off without making at least one individual worse off.) In the phase diagram for the lattice model, this balance occurs in a narrow region at the boundary between the regions dominated by pests and water (*SI Appendix*, Fig. S4). The resulting distribution of colored patches (synchronized irrigation schedules) on the lattice is readily comparable with the satellite imagery.

Comparison with Satellite Imagery

We analyzed patch distributions in six rice-growing regions, randomly selected on the basis of absence of cloud cover (Fig. 1*A*). Fig. 1*B* shows one of these regions (Gianyar) on a particular observation day. Four different phases of rice growth corresponding to the irrigation schedules are clearly visible in the multispectral and panchromatic satellite images: growing rice, harvest, flooded, and drained. Image analysis is based on measuring photosynthetic activity; see *Methods* and *SI Appendix*. Fig. 1*C* shows the cumulative distribution function (red circles) of the patch sizes s, as they are found in Fig. 1*B* (Gianyar region). It shows a power-law distribution $P(> s) \propto s^{-\alpha}$ with a tail exponent of $\alpha = 0.93(0.07)$; the SE is given in brackets. The patch size distributions for all other regions at all observation times are shown in Fig. 1*C*, *Inset*; corresponding exponents are fitted from the data with a standard maximum likelihood estimator (see *SI Appendix*) and are listed in *SI Appendix*, Table S2.

The cumulative patch size distribution is visible in the power law (Fig. 1*C*). The model results (blue squares) for the phase transition (when $b/a \approx 20$ at $t = 400$) closely matches the empir-

ical data (red circles), and would be very similar at $t = 10$. Similar agreement occurs in the correlation function $C(d)$. For the appropriately scaled model results (to match the length scales in the satellite images and the model dimension), we find very similar functional dependence of the correlation function in Fig. 1*D*. Both data and model show an approximate power-law decay in the correlation function.

Correlation functions $C(d)$ provide a second measure of the scale of cooperation among farmers. In Fig. 1*D* (red) for Gianyar, we see that correlation functions decay slowly with distance: The closer two patches are, the more likely they are to follow the same irrigation schedule, indicating that all patches are linked. Correlation functions decline as a power law. Thus, the state of each patch affects all of the others, and the Gianyar rice terraces form an integrated (globally coupled) system; Fig. 1*D*, *Inset* shows that this is true for all regions and observations. To quantify the typical correlation length, we define it as the variance of the correlation function; see Eq. **2** in *Methods*. For Gianyar, the correlation length turns out to be $\varepsilon = 373$ m, spanning all patches. The results for the other regions are found in *SI Appendix*, Table S2.

We performed a systematic study of the dependence of the average harvests H, the power-law exponents α, and the correlation lengths ε on the parameters a and b. The results are shown in Fig. 4. Here, we observe the emergence of critical behavior at a region where water stress and pest stress balance as adaptation progresses in the simulation. This region is highlighted with white lines in Fig. 4*B*. A comparison with the observed data for the power-law exponent α in *SI Appendix*, Table S2 suggests that model results from this parameter region are compatible with the empirical data. At the critical region, the entire system of farms becomes correlated as global control emerges from simple local interactions between farmers.

Discussion

We suggest that the dynamics captured in the lattice model described above show that self-organized criticality (SOC) can emerge from an adaptive process. The evidence that this finding tells us something about the Balinese subak system is based on the remarkable similarity of the distributions of patch sizes and correlation distances in the satellite imagery and the model. However, power-law distributions can occur for many reasons. For example, they often occur in vegetation patches in dryland ecosystems under stress (5–8). However, vegetation patches in natural ecosystems are functionally similar, differing only in size. For the vegetation patches that make up the mosaics of the rice terraces, size matters, but so does the age of the rice crop in each patch, which depends on the irrigation schedules selected by the farmers. Any explanation for the observed power-law distribution of patches in the rice terraces needs to account for this functional coupling of irrigation schedules and ecosystem dynamics. Our adaptive SOC model tests the hypothesis that the observed mosaic patterns might arise from the farmers' efforts to optimize the pest–water trade-off. The model shows that, if the adaptive dynamics are driven by the pest–water trade-off, there exist critical points where the power-law distribution is the attractor. Because approximate Pareto optimality emerges at this point, where the pest–water trade-off is optimized at all scales, the model also suggests an explanation for the historical persistence of this attractor. For these reasons, we suggest that the emergence of power-law mosaics is not a purely biological phenomenon but is the outcome of ongoing coupled human–natural dynamical interactions. Two further assumptions of the model can be evaluated with historical data.

First, the model assumes that subaks actively cooperate to minimize losses due to pests and water shortages by synchronizing their irrigation schedules. This assumption can be evaluated in light of historical evidence. From the ninth to the 14th
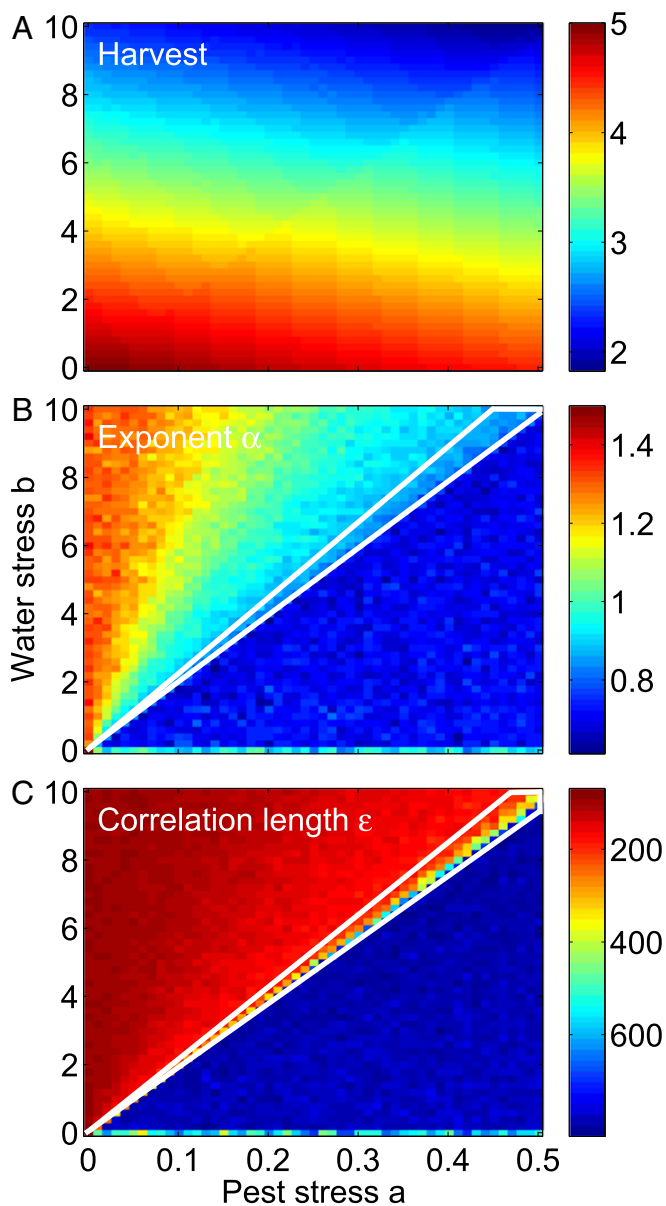
Fig. 4. Effects of pest and water stress: model results as a function of parameters *a* (pests) and *b* (water). (*A*) Average harvests. The maximum possible harvest H_0 occurs when $a = b = 0$. (*B*) Power-law exponent α of the cumulative patch size distribution. The parameter region that matches the observed slopes from the satellite imagery (*SI Appendix*, Table S2) is indicated by the white line. (*C*) Correlation length ε. The parameter region that matches the observed slopes from the satellite imagery (*SI Appendix*, Table S2) is found around the line where $b/a \approx 20$, which is indicated with the white line. Further computations show the same critical behavior at $b/a \approx 14$ when $m = 0.2$, or at $b/a \approx 24$ for $m = 0.05$ (see *SI Appendix*, Fig. S2). Thus, the emergence of critical behavior does not depend simply on *a* and *b* but also on the constant *m* in the denominator of pest stress. In conclusion, taking results from exponents and correlation lengths, the parameter region that is compatible with observations is $b/a \approx 20$. Simulations were performed with $L = 100$, $r = 2$, $f = 0.05$, and $N = 4$.

centuries AD, numerous royal inscriptions encouraged villagers to construct irrigation systems, and left water management in their hands (9). Because of Bali's steep volcanic topography, "the spatial distribution of Balinese irrigation canals, which by their nature cross community boundaries, made it impossible for irrigation to be handled at a purely community level" (10). Later on, both Balinese and European manuscripts describe coopera-

tive management by the subaks. Soon after the final conquest of Bali by the Dutch in 1908, the colonial irrigation engineer tasked with surveying Balinese irrigation wrote "if due to lack of water not all areas can get water, then they create a turn-taking which is decided upon during the monthly meetings" (11).

Second, the model predicts that rice yields will be optimized by irrigation schedules that balance the pest–water trade-off for multisubak groups. This prediction was inadvertently tested by the introduction of Green Revolution agriculture to Bali in the 1970s. At that time, the subaks were required to give up the right to set their own irrigation schedules. Instead, each farmer was instructed to cultivate Green Revolution rice as often as possible, resulting in unsynchronized planting schedules. By 1977, 70% of southern Balinese rice terraces were planted with Green Revolution rice. At first, rice harvests increased. Within 2 y, however, Balinese agricultural and irrigation workers reported "chaos in water scheduling" and "explosions of pest populations" (ref. 3, p. 114). In 1985, the Department of Public Works in Tabanan (the largest rice-growing regency in Bali) reported that "the following factors caused the explosion of pests and diseases: 1. In areas with sufficient irrigation water, farmers are now planting continuously throughout the year. 2. In areas with insufficient water, farmers are planting without a coordinated schedule. In other words, the farmers/subaks have ceased to follow the centuries-old cyclical cropping patterns" (12). It was only when farmers spontaneously returned to synchronized planting schemes that harvests began to recover, a point subsequently acknowledged by the final evaluation team from the Asian Development Bank (13).

Why was the functional significance of multisubak cooperation not apparent to the Green Revolution planners? The model suggests a possible explanation. Power-law distributions of dryland vegetation are comparatively obvious because the patches differ only in size. However, adaptive management by the subaks creates differentiated patches of varying size. The distinction is significant, not only because similar versus differentiated patches occur for different reasons but also because it is harder for observers to detect the connectivity of differentiated patches. Perhaps partly for this reason, until now theoretical models of coupled human–natural systems like rice terraces have not anticipated or accounted for the emergence of global-scale connectivity, focusing instead on local interactions. The model also suggests an explanation for the widespread occurrence of fragile kilometers-long irrigation systems linking multiple subaks in the mountains of Bali. If management by the subaks were purely local, leaving downstream subaks at the mercy of their upstream neighbors, these irrigation works would be pointless, and the total area of terraced fields on the island could never have reached its historic extent (14).

In retrospect, it is not surprising that the concept of SOC is relevant to the emergence of cooperation in human interactions with ecosystem processes. Models of SOC were developed to understand how small-scale local interactions can transit to integrated global connectivity, popularized by the compelling sandpile example (15). These models often behave as if operating exactly at a phase transition. There, the systems become "critical," which means that correlations become long-range, and effectively span the entire system, even though interactions only happen at the local nearest-neighbor level.

In the subak lattice model, realistic configurations of patches appear after just a few simulation steps. At the same time, harvests approach Pareto optimality (if any farmer changes his irrigation pattern, his rice harvests or those of other farmers will decline). The total harvest of all farms is also maximized. The subak model does not evolve to full alignment of behavior (except when $b = 0$), which would minimize pest losses but maximize water stress. Instead, at the critical point, the adaptive update process of farmers continues to a point where

correlations span the entire system. For this reason, we call the model dynamics "adaptive SOC."

We conclude with the question of whether these results are likely to be unusual, perhaps even unique to Bali. The scope of the model is limited by the physical geography of Bali. The four crater lakes store rainfall that feeds the groundwater system, but they have no river outlets. On the steep porous volcanic slopes, rivers recharge very quickly. Irrigation systems consist of one to six closely spaced weirs and springs that provide water for one or more subaks. These local irrigation systems are functionally independent: Although they remove most or all of the flow, a kilometer or two downstream, it will be replenished from groundwater flows. Our model captures the adaptive process at this scale, where local groups of farmers meet face to face to solve the pest–water trade-off. The concept of emergent global-scale connectivity in our model, which we borrow from physics, does not refer to all of the subaks on a river but to these smaller functionally independent groups of subaks, such as those shown in Fig. 1*B* and *SI Appendix*, Figs. S3 and S6–S17. This configuration of water distribution contrasts with a typical desert river, where the effects of upstream irrigation may be felt far downstream.

If several subaks share water resources, their elected leaders meet to negotiate irrigation schedules. Although this higher-level coordination between subaks is not explicitly included in the model, the decision-making process is the same: a trial-and-error adaptation to reduce pest and water stress. These meetings take place in regional water temples and make use of a sophisticated permutational calendar to plan and implement staggered irrigation schedules (14, 16). These cultural innovations undoubtedly facilitate adaptation to changing pest–water dynamics. However, the model does not require calendars or water temples; instead, it helps to clarify the functional significance of these social constructs for sustaining approximate Pareto optimality. Our model shows that the simple pest–water trade-off triggers continuous transitions that turn adaptive agents on a two-dimensional lattice into a coevolving system capable of solving the pest–water trade-off by means of local decision-making. Unlike Gunderson and Holling's well-known model of adaptive cycles (17), here increasing connectivity does not cause collapse but stabilizes at a scale-free distribution of functionally varied patches. This is quite a general result that may be common in coupled human–natural systems. In any anthropogenic landscape, correlations between patches will provide some information about the scale of human management (see *SI Appendix* for code). If Bali's subaks are not unique, and adaptive SOC occurs in the management of the commons elsewhere, it should be readily detectable from correlated patch distributions.

Methods

Correlation Functions. We use a definition of correlation function $C(d)$ that is based on the mutual information between the cropping pattern X at site i and the cropping pattern Y at site j, where the distance from site i to j is d. The mutual information measures how much the knowledge of the cropping pattern at one site reduces the uncertainty on the knowledge of the cropping pattern at the other site. It is defined as

$$C(d) = \frac{1}{\mathcal{N}} \sum_{X=1}^{4} \sum_{Y=1}^{4} P_d(X, Y) \log_2 \frac{P_d(X, Y)}{P_d(X) P_d(Y)},$$ [1]

where $P_d(X, Y)$ is the probability of cropping patterns X and Y occurring at sites that are a distance d apart. Note that X and Y take values from 1 to 4 with '1 = green', '2 = red', '3 = blue' and '4 = yellow'. Operationally, the joint probability $P_d(X, Y)$ is determined by taking the relative frequency of the cropping patterns X and Y against all possible combinations of cropping patterns between sites at a relative distance d. Note that the site here refers either to a pixel in the satellite image or to a lattice site for the model. The marginal probability of cropping pattern X (or Y) is $P_d(X)$ [or $P_d(Y)$]. $\mathcal{N}$ is the normalization constant. It is equal to the Shannon entropy of the cropping pattern X, i.e., $\mathcal{N} = -\sum_{X=1}^{4} P_0(X) \log_2 P_0(X)$. It ensures that the correlation is normalized, so that $C(d = 0) = 1$. We use this definition for the correlation function because it is applicable to random variables in symbolic form. The standard correlation function in two dimensions is inappropriate, as it needs random variables in numeric form. However, these two definitions for the correlation functions are closely related if the joint probability distribution is Gaussian (18).

Correlation Length. The correlation length ε is defined as the variance (second moment) of the correlation function from Eq. **1**,

$$\varepsilon = \left(\frac{\sum_d d^2 C(d)}{\sum_d C(d)} \right)^{\frac{1}{2}}.$$ [2]

1. Lansing JS, Cox MP, Downey SS, Jannsen MA, Schoenfelder JW (2009) A robust budding model of Balinese water temple networks. *World Archaeol* 41:112–133.
2. Lansing JS, Miller JH (2005) Cooperation, games, and ecological feedback: Some insights from Bali. *Curr Anthropol* 46:328–334.
3. Lansing JS (1998) *Priests and Programmers: Technologies of Power in the Engineered Landscape of Bali* (Princeton Univ Press, Princeton, NJ).
4. Lansing JS (2006) *Perfect Order: Recognizing Complexity in Bali* (Princeton Univ Press, Princeton, NJ).
5. Solé RV, Manrubia SC (1995) Self-similarity in rain forests: Evidence for a critical state. *Phys Rev E* 51:6250–6253.
6. Pascual M, Guichard F (2005) Criticality and disturbance in spatial ecological systems. *Trends Ecol Evol* 20:88–95.
7. Kéfi S, et al. (2011) Robust scaling in ecosystems and the meltdown of patch size distributions before extinction. *Ecol Lett* 14:29–35.
8. Kéfi S, Holmgren M, Schaffer M (2016) When can positive interactions cause alternative stable states in ecosystems? *Funct Ecol* 30:88–97.
9. Scarborough V, Schoenfelder JW, Lansing JS (2000) Early statecraft on Bali: The water temple complex and the decentralization of the political economy. *Res Econ Anthropol* 20:299–330.

10. Christie JW (2007) *A World of Water: Rain, Rivers and Seas in Southeast Asian Histories* (KITLV Press, Leiden, The Netherlands) pp 235–258.
11. van Naerssen E (1918) Irrigatie en waterverdeeling volgens de Opvatting der Baliërs. *Adatrechtbundel* 15:27–39.
12. Tukiman (1985) *Pengalaman dalam Merumuskan Pola Tanam di Kabupaten DATI II Tabanan [Experience of Formulating a Cropping Pattern for the Tabanan Regency]* (Irrig Div, Gov Bali, Denpasar, Bali), Jalan Beliton 2, p 1.
13. Asian Development Bank (1992) *Project Performance Audit Report, Bali Irrigation Sector Project* (Asian Dev Bank, Mandaluyong, Philippines), L-522-INO.
14. Lansing JS, De Vet T (2012) The functional role of Balinese water temples: A response to critics. *Hum Ecol* 40:453–467.
15. Bak P (1996) *How Nature Works: The Science of Self-organized Criticality* (Copurnicus, New York).
16. Lansing JS, et al. (2014) Regime shifts in Balinese subaks. *Curr Anthropol* 55: 232–239.
17. Gunderson LH, Holling CS (2001) *Panarchy: Understanding Transformations in Human and Natural Systems* (Island Press, Washington, DC).
18. Fraser AM (1989) Reconstructing attractors from scalar time series: A comparison of singular system and redundancy criteria. *Phys D* 34:391–404.